# Optical antennas direct single-molecule emission

T. H. TAMINIAU[1], F. D. STEFANI[1], F. B. SEGERINK[2] AND N. F. VAN HULST[1,3]*

[1]ICFO — Institut de Ciencies Fotoniques, Mediterranean Technology Park, 08860, Castelldefels (Barcelona), Spain
[2]Optical Sciences Group, MESA+ Institute for NanoTechnology, University of Twente, PO Box 217, 7500AE Enschede, The Netherlands
[3]ICREA — Institució Catalana de Recerca i Estudis Avançats, 08015 Barcelona, Spain
*e-mail: Niek.vanHulst@ICFO.es

Published online: 16 March 2008; doi:10.1038/nphoton.2008.32

**Antennas have been used for more than a century to control the emission and collection of radio and microwave radiation[1]. An optical analogue is of great interest as it will allow unique control of absorption and emission[2,3] at the nanometre scale[4]. Despite the intense recent research on optical antennas[5–8], one of the main functions of traditional antennas, the directing of radiation, remains a challenge at optical frequencies. Here we experimentally demonstrate control of the emission direction of individual molecules by reversible coupling to an optical monopole antenna. We show how the angular emission of the coupled system is determined by the dominant antenna mode—that is, the antenna design—regardless of molecular orientation. This result reveals the role of the plasmon mode in the emission process and provides a clear guideline how to exploit the large available library of radio antennas to direct emission in nano-optical microscopy[9,10], spectroscopy[11,12] and light-emitting devices, including single-photon sources[13–15].**

Control of the emission of quantum systems, such as fluorescent molecules, atoms or quantum dots, is subject to intense research[16–18]. The emission direction, spectrum and lifetime depend on the electromagnetic (vacuum) field[2] and can thus be controlled by shaping the photonic environment[3].

Photonic crystals[16,19], dielectric spheres[17], other cavities[14,18] and metallic surfaces[20] have been explored with a view to modifying the field. In contrast, more localized modifications exist at metallic nanoparticles, which support plasmon resonances. Such particles function, in a way that is analogous to resonant radio antennas, as optical antennas[4–8]. In reception, they efficiently confine optical fields in subdiffraction-limited volumes[6–8]. By reciprocity, optical antennas will allow nanoscale control of lifetime[5,21,22], spectrum and, as demonstrated here, the direction of photon emission.

To understand how the emission direction can be controlled, we first consider a basic example. The angular emission of the elementary hertzian dipole in free space is the familiar 'doughnut' pattern (Fig. 1a). The resonant dipole antenna, with a length of half the effective wavelength[23], has a radiation pattern qualitatively similar to that of the dipolar emitter. If a horizontal emitter is coupled to a vertical antenna, by placing it at a point of high electric mode density, a new angular emission pattern is observed (Fig. 1b). The pattern is rotated compared with the free dipole and instead resembles the antenna radiation pattern. For the radiation patterns in Fig. 1, the origin is placed at the calculated apparent phase centre[24], the point from which the radiation is seen to emanate. Interestingly, for the coupled system the phase centre is located at the middle of the antenna. It is thus difficult to determine the exact location or orientation of the original dipole source from the far-field radiation, unless its position can be varied controllably. These example calculations suggest that for the coupled system the antenna is in fact the main radiator.

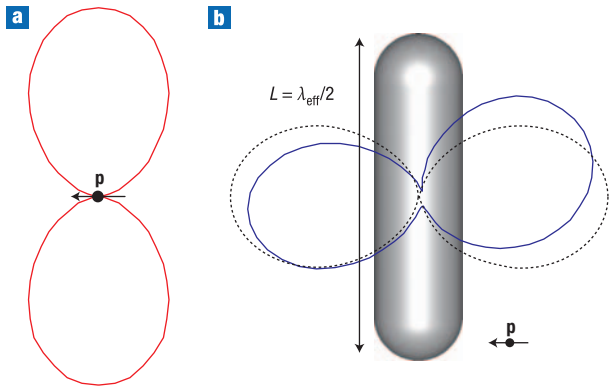


**Figure 1 Emission control with a dipole antenna. a**, Angular emission of a horizontal radiating dipole (**p**) in free space. **b**, Angular emission of the same dipole coupled to a vertical dipole antenna (blue), which has a length, $L$ equal to half the effective wavelength at resonance, $\lambda_{eff}$, is dominated by the antenna (black dotted) (see ref. 29 for FIT calculations).

In practice, complete control of angular emission requires the direct observation and manipulation of the interaction of a single emitter with a suitable antenna. For an ensemble of emitters[25], any induced changes in angular emission of individual dipole transitions can simply not be separated from enhanced excitation or emission rates of favourably oriented dipoles. As for the antenna, it needs to have a well-defined radiation pattern, that is, a fixed preferential dipole (or higher order) moment and a resonance at optical frequencies. This explains why previous experiments for single emitters close to gold spheres[5] and near-field probes[26] have only shown minor, often not understood[26] effects; a sphere does not have a preferential dipole orientation,

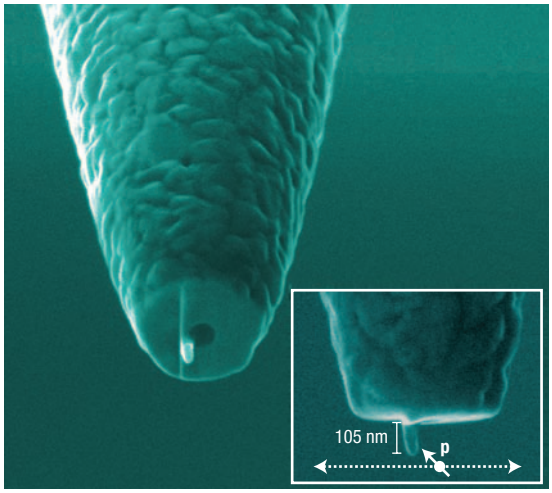


**Figure 2 Optical monopole antenna.** An aluminium nano-antenna (SEM image viewed from an angle of 52°) was sculpted with a focused ion beam at the end face of an aperture near-field fibre probe (see Methods and ref. 27). The antenna length was controlled to tune the antenna plasmon resonance. For the example shown, the antenna length was 105 nm. The typical antenna width was 40 nm and the radius of curvature at the apex was 20 nm. The inset shows a side view and schematically depicts the emitter, a single fluorescent molecule, its transition dipole moment (**p**) and its movement in the experiment.

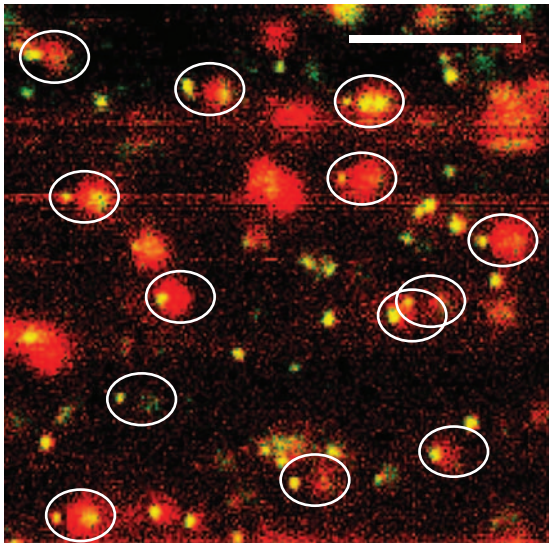

**Figure 3 Single-molecule fluorescence.** Spatial fluorescence map obtained by scanning a sample containing randomly placed isolated single fluorescent molecules under the antenna. The excitation ($\lambda_{exc} = 514$ nm) polarization is horizontal. The emitted fluorescence ($\lambda_{em} \sim 570$ nm) is split into two polarization components. The horizontal polarization is coloured red, vertical polarization is green; yellow corresponds to a balance of equal horizontal and vertical polarization. Examples of patterns originating from one single molecule are circled. The change of colour within one pattern indicates that the emission of a single molecule is modified as it is scanned around the antenna. The scale bar indicates 1 μm.

and the probe does not support any clear resonant modes. The probe-based nano-antenna of Fig. 2 fulfils the criteria. A preferred dipole moment is fixed along the long antenna axis. The resonance is tuned to optical frequencies by controlling the antenna length. The field modes and resonances are characteristic for a monopole antenna[8], half a dipole antenna with the other half replaced by the reflection in a ground plane. For all purposes, such an antenna can be modelled to a good approximation as a dipole antenna.

Fluorescent molecules were used as dipolar single emitters. Spatially isolated DiI (1,1′-dioctadecyl-3,3,3′,3-tetramethylindocarbocyanineperchlorate) molecules were immobilized in a 20-nm-thick polymethylmethacrylate (PMMA) layer on a glass substrate (see Methods). The experiments were performed at room temperature. The molecular position, and thus the coupling to the antenna, was controlled using a scanning probe microscope. The molecules were raster-scanned under the antenna while a constant antenna–sample distance was maintained using a shear-force feedback system (Fig. 2, inset). The antenna was used both to excite the molecules (wavelength of excitation $\lambda_{exc} = 514$ nm) and to mediate the emission (wavelength of emission $\lambda_{em} \approx 570$ nm). For excitation, the antenna mode was fed through the aperture of the probe[10] by coupling a laser beam of controlled polarization into the fibre[8]. The emitted single-molecule fluorescence was collected by a 1.3-numerical-aperture (-NA) objective below the sample. Finally, to characterize the angular emission, the fluorescence was split by a polarizing beam splitter into two perpendicular polarization components, each detected by a separate avalanche photodiode.

As each molecule was scanned under the antenna, the fluorescence intensity mapped the component of the local excitation field oriented along the molecular transition dipole[9,28]. Distinct small (full-width at half-maximum (FWHM) $\approx 30$ nm) and larger (FWHM $\geq 100$ nm) bright spots are present in the resulting images. Recurring patterns consisting of a small spot accompanied by a large spot on the right are visible (Fig. 3). The small spots are the responses of single molecules excited by the antenna. Their small dimension (only 30 nm) demonstrates the nanoscale interaction with the antenna mode. The larger spots are the molecular responses to the residual field of the aperture at the right side of the antenna. One such pattern is thus the response of one single molecule. This is one of the key points of the experiment: the fluorescence of a single molecule is monitored as it is coupled (small spot in the data) and uncoupled (large spot) to the antenna.

The property of interest is the detected emission polarization, which is colour coded: red is horizontal, green is vertical. The polarization is clearly not uniform within one single-molecule pattern. The small spots are mostly yellow, indicating equal intensity in both polarization channels. The large spots are mainly horizontally polarized (red), reflecting the preferential excitation of molecules with a transition dipole oriented along the horizontal excitation polarization[9,28]. The molecular emission is indeed modified as the molecule is scanned near the antenna.

To interpret the effect of the antenna on the molecular emission, full three-dimensional finite-integration technique[29] (FIT) electromagnetic-field calculations were performed. The antenna was modelled as a dipole antenna, resonant at the emission wavelength of 570 nm (Fig. 4a). Realistic material parameters were used and the glass substrate was included. The molecule was represented by a hertzian dipole, oscillating at the emission frequency. It is illustrative to consider the case of an $x$-oriented molecule, as the antenna effect is most prominent for an orientation perpendicular to the antenna. The far-field radiation patterns for a selection of distances from the antenna are shown in Fig. 4d. Far from the antenna ($x = 500$ nm), the

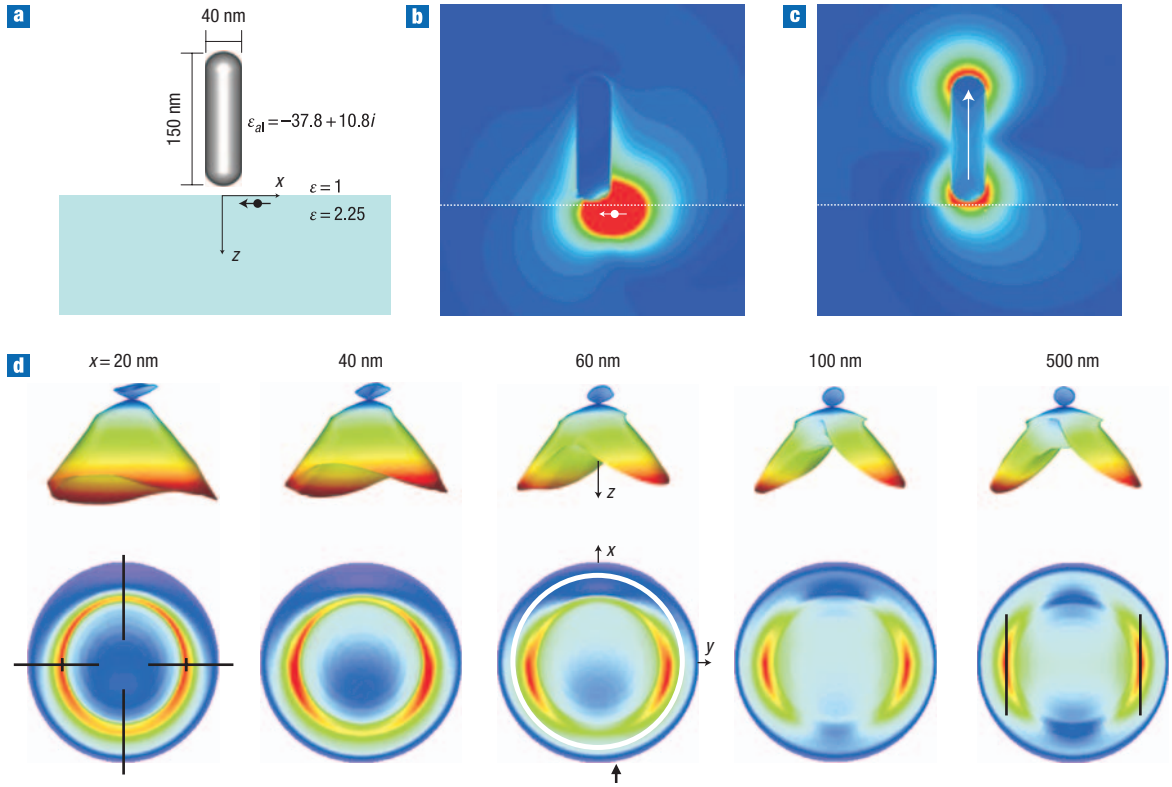


**Figure 4 The electromagnetic field of a dipole emitter near the antenna. a**, Overview of the FIT calculations. The antenna is placed 4 nm above the sample. The dipole emitter is embedded in the sample 6 nm below the surface a distance $x$ away from the antenna axis ($\lambda_{em} = 570$ nm). Results for an $x$-oriented dipole are shown. **b**,**c**, Instantaneous local electric field amplitude for two different phases ($\varphi$) where $x = 20$ nm. In **b** the field of the dipole emitter is maximum ($\varphi = 0°$), and in **c** the antenna response is resonant ($\varphi = 90°$). Red indicates high field amplitude. **d**, Far-field emission for different distances ($x$). The top row shows three-dimensional radiation intensity patterns. The bottom row presents the intensity in the back focal plane. The white circle in the middle image encloses the emission detected with the NA = 1.3 objective used in the experiments. The magnitude of the contributions polarized along $x$ and $y$ of the main lobes is marked in black for $x = 20$ and $x = 500$ nm (black lines).

molecular emission into the glass consists of two lobes, as expected for a dipole oriented parallel to a dielectric interface in the absence of the antenna[30]; that is, the emission is unperturbed. As the molecule approaches the antenna, the radiation pattern gradually changes. At $x = 20$ nm, where the coupling is maximum, the pattern resembles a cone. Such a pattern is characteristic for a dipole perpendicular to a dielectric interface[30]. As in the example of Fig. 1, the coupled system emits like a dipole oriented parallel to the antenna axis.

More insight can be gained by considering the local field dynamics at the coupled system ($x = 20$ nm). At resonance, the antenna response is a standing wave nearly 90° out of phase with the driving field of the dipole emitter. By taking two snapshots of the field, a quarter of a field cycle apart, the local contributions of the emitter (Fig. 4b) and the antenna (Fig. 4c) are visualized separately (for the full cycle, see Supplementary Information, Video 1). Both contributions are dipolar and oriented perpendicular to each other. The emitter near-field couples to the dipolar antenna plasmon resonance, which in turn couples to the radiation field.

To relate the calculations to the experiment, the intensity and polarization in the back focal plane of the objective were calculated (Fig. 4d). For the coupled system ($x = 20$ nm), the intensity distribution is nearly circular and the polarization approximately radial; that is, equal intensity is detected in each polarization channel. Indeed, in Fig. 3 the emission polarization of single molecules coupled to the antenna (small spots) is mostly 'yellow'. In the uncoupled case ($x > 100$ nm), the intensity distribution is highly asymmetric and the polarization depends strongly on the molecular orientation, as observed for the molecules under the aperture (large spots). The angular emission of the coupled and uncoupled systems can thus be distinguished by the polarization in the back focal plane.

For a quantitative comparison of the experiment to the calculations, we define the degree of polarization (DOP) as

$$\mathrm{DOP} = (I_r - I_g)/(I_r + I_g),$$

where $I_r$ and $I_g$ are the intensities in the red and green polarization channels, respectively. The DOP was obtained for each molecule in the experiments, when coupled and uncoupled to the antenna. The same two DOPs were taken from calculations for a large number of randomly oriented molecules. Figure 5 plots the coupled DOP against the uncoupled DOP. The experimental data are in excellent agreement with the calculated results. As a reference the identity line for the situation without antenna is plotted. The clear deviation of the results from that line illustrates the strong influence of the antenna. The coupled DOP values lie close to zero. This is the expected value for the antenna dipole emission; the coupled system indeed emits like the antenna mode. The slight asymmetric deviation from zero, observed both in the

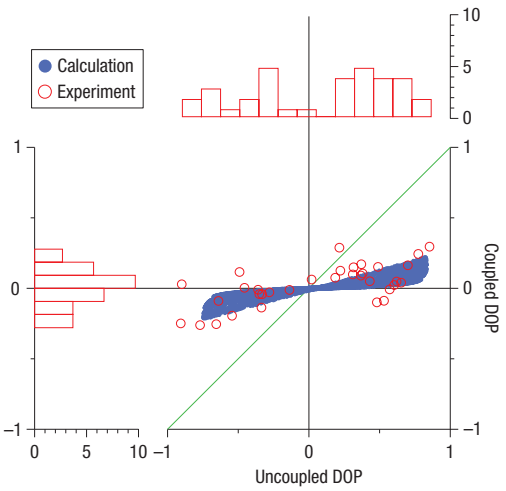


**Figure 5 Control of angular emission with an optical monopole antenna.** The degree of polarization for molecules coupled to the antenna versus the DOP for the same molecules uncoupled. The 34 experimental values are a compilation obtained for various antennas and different excitation polarizations. The coupled DOP value is centred on zero, the expected value for the antenna emission.

experiment and calculations, is due to the finite coupling strength. For the same molecules, the values for the uncoupled DOP are spread all through the theoretical range (−0.8 to 0.8 for a 1.3 NA objective), indicating that molecules of many different orientations are probed. Thus these results prove that, regardless of the molecular orientation, the emission pattern for molecules coupled to the antenna is determined by the antenna radiation pattern.

In conclusion, we have experimentally demonstrated the control of emission direction of a single emitter by an optical antenna. The principle is straightforward; the angular emission of the coupled system is determined by the antenna emission. This result gives a clear guideline how to incorporate the large library of radiowave antenna designs into nano-optics. Moreover, it gives direct experimental insight into the role of the plasmon mode[4]: the emitter couples to the antenna plasmon mode (reducing the excited-state lifetime[5]), which in turn couples to the radiation field (determining the angular emission). The strong redirection of emission observed can severely modify the detection efficiency in nanoparticle-emitter experiments. Finally, we predict that combining control of angular emission and transition rates in suitably designed optical antennas will lead to full control of absorption and emission at the nanoscale.

## METHODS

### ANTENNA FABRICATION

The probes were fabricated following the methods of ref. 27. Single-mode (operating at a wavelength, $\lambda = 633$ nm) fibres were heat pulled with a SUTTER P2000 fibre puller so that two probes with a 100-nm-diameter end face were formed. Probes were coated, while rotating, with a 2-nm-thick chromium adhesion layer (0.1 nm $s^{-1}$) and a 150-nm-thick aluminium layer (1 nm $s^{-1}$) by electron-beam evaporation. An elongated antenna, next to a circular aperture, was formed in a two-step focused-ion-beam milling process from the side. The antenna lengths used ranged from 75 nm to 90 nm ($\pm$10 nm) (for the dipole in the calculations the length was doubled). The probes were glued onto a quartz tuning fork for shear-force feedback.

### SAMPLE FABRICATION

First, 0.5% PMMA was dissolved in toluene. Carbocyanine (DiIC18) dye molecules were added at a $1 \times 10^{-8}$ molar concentration. The solution was spin coated onto plasma-etched glass substrates. Samples were dried at ambient conditions.

### FINITE-INTEGRATION-TECHNIQUE CALCULATIONS

Calculations were performed with the transient FIT solver of CST Microwave Studio. The electronic molecular transition was approximated as a pure electric dipole and represented by a classical dipole of constant oscillator strength.

Received 11 October 2007; accepted 25 January 2008; published 16 March 2008.

## References

1. Hertz, H. Űber electrodynamische Wellen im Luftraume und deren Reflexion. *Annalen der Physik und Chemie* **270,** 609–623 (1888).
2. Fermi, E. Quantum theory of radiation. *Rev. Mod. Phys.* **4,** 87–132 (1932).
3. Purcell, E. M. Spontaneous emission probabilities at radio frequencies. *Phys. Rev.* **69,** 681 (1946).
4. Greffet, J.-J. Nanoantennas for light emission. *Science* **308,** 1561–1563 (2006).
5. Kühn, S., Håkanson, U., Rogobete, L. & Sandoghdar, V. Enhancement of single-molecule fluorescence using a gold nanoparticle as an optical nanoantenna. *Phys. Rev. Lett.* **97,** 017402 (2006).
6. Fromm, D. P., Sundaramurthy, A., Schuck, J., Kino, G. & Moerner, W. E. Gap-dependent optical coupling of single 'Bowtie' nanoantennas resonant in the visible. *Nano Lett.* **4,** 957–961 (2004).
7. Mühlschlegel, P., Eisler, H.-J., Martin, O. J. F., Hecht, B. & Pohl, D. W. Resonant optical antennas. *Science* **308,** 1607–1609 (2005).
8. Taminiau, T. H., Moerland, R. J., Segerink, F. B., Kuipers, L. & van Hulst, N. F. $\lambda/4$ resonance of an optical monopole antenna probed by single molecule fluorescence. *Nano Lett.* **7,** 28–33 (2007).
9. Betzig, E. & Chichester, R. J. Single molecules observed by near-field scanning optical microscopy. *Science* **262,** 1422–1425 (1993).
10. Frey, H. G., Witt, S., Felderer, K. & Guckenberger, R. High-resolution imaging of single fluorescent molecules with the optical near-field of a metal tip. *Phys. Rev. Lett.* **93,** 200801 (2004).
11. Nie, S. & Emory, S. R. Probing single molecules and single nanoparticles by surface-enhanced Raman scattering. *Science* **275,** 1102–1106 (1997).
12. Hartschuh, A., Sánchez, E. J., Xie, X. S. & Novotny, L. High-resolution near-field Raman microscopy of single-walled carbon nanotubes. *Phys. Rev. Lett.* **90,** 095503 (2003).
13. Kim, J., Benson, O., Kan, H. & Yamamoto, Y. A single-photon turnstile device. *Nature* **397,** 500–503 (1999).
14. Michler, P. *et al.* A quantum dot single-photon turnstile device. *Science* **290,** 2282–2285 (2000).
15. Lounis, B. & Moerner, W. E., Single photons on demand from a single molecule at room temperature. *Nature* **407,** 491–493 (2000).
16. Lodahl, P. *et al.* Controlling the dynamics of spontaneous emission from quantum dots by photonic crystals. *Nature* **430,** 654–657 (2004).
17. Schniepp, H. & Sandoghdar, V. Spontaneous emission of europium ions embedded in dielectric nanospheres. *Phys. Rev. Lett.* **89,** 257403 (2002).
18. Steiner, M. *et al.* Microcavity-controlled single-molecule fluorescence. *Chem. Phys. Chem.* **6,** 2190–2196 (2005).
19. Hennessy, K. *et al.* Quantum nature of a strongly coupled single quantum dot-cavity system. *Nature* **445,** 896–899 (2007).
20. Wedge, S. & Barnes, W. L. Surface plasmon-polariton mediated light emission through thin metal films. *Opt. Express* **12,** 3673–3685 (2004).
21. Anger, P., Bharadwaj, P. & Novotny, L. Enhancement and quenching of single-molecule fluorescence. *Phys. Rev. Lett.* **96,** 113002 (2006).
22. Farahani, J. N., Pohl, D. W., Eisler, H.-J. & Hecht, B. Single quantum dot coupled to a scanning optical antenna: A tunable superemitter. *Phys. Rev. Lett.* **95,** 017402 (2005).
23. Novotny, L. Effective wavelength scaling for optical antennas. *Phys. Rev. Lett.* **98,** 266802 (2007).
24. Balanis, C. A. *Antenna Theory: Analysis and Design* 3rd edn 799–801 (Wiley, Hoboken, New Jersey, 2005).
25. Mertens, H., Biteen, J. S., Atwater, H. A. & Polman, A. Polarization-selective plasmon-enhanced silicon quantum-dot luminescence. *Nano Lett.* **6,** 2622–2625 (2006).
26. Gersen, H. *et al.* Influencing the angular emission of a single molecule. *Phys. Rev. Lett.* **85,** 5312–5315 (2000).
27. Veerman, J. A., Otter, A. M., Kuipers, L. & van Hulst, N. F. High definition aperture probes for near-field optical microscopy fabricated by focused ion beam milling. *Appl. Phys. Lett.* **72,** 3115–3117 (1998).
28. Veerman, J. A., Garcia-Parajo, M. F., Kuipers, L. & van Hulst, N. F. Single molecule mapping of the optical field distribution of probes for near-field microscopy. *J. Microsc.* **194,** 477–482 (1999).
29. Weiland, T. Discretization method for solution of Maxwells equations for 6-component fields. *Electron. Commun. AEU* **31,** 116–120 (1977).
30. Lukosz, W. Light-emission by magnetic and electric dipoles close to a plane dielectric interface. III. Radiation patterns of dipoles with arbitrary orientation. *J. Opt. Soc. Am.* **69,** 1495–1503 (1979).

## Acknowledgements

We thank J. Overman for performing the initial experiments, L. Kuipers and R.J. Moerland for discussions, Computer Simulation Technology (CST), Darmstadt, Germany, for constructive feedback on the use of Microwave Studio, and the Koerber Foundation (Hamburg, Germany) for financial support. Correspondence and requests for materials should be addressed to N.F.v.H.
Supplementary information accompanies this paper on www.nature.com/naturephotonics.

## Author contributions

T.H.T. performed the experiments, carried out the interpretation and wrote the manuscript. F.D.S. and T.H.T. performed and processed the FIT calculations. F.B.S. and T.H.T. fabricated the antennas. N.F.v.H. supervised the project.